Novel pyrrolecycloalkylpyrazole analogs as CB1 ligands.

Battistina Asproni[a,*], Ilaria Manca,[b] Giansalvo Pinna,[a] Elena Cichero[c], Paola Fossa[c], Gabriele Murineddu[a], Paolo Lazzari[b], Giovanni Loriga[d], Gérard A. Pinna[a].

[a] *Dipartimento di Chimica e Farmacia, Università degli Studi di Sassari, Via F. Muroni 23/a, 07100 Sassari, Italy*

[b] *KemoTech Srl, Edificio 3, Loc. Piscinamanna, 09010 Pula, CA, Italy*

[c]*Dipartimento di Farmacia, Università di Genova, Viale Benedetto XV n. 3, 16132, Genova, Italy*

[d]*Consiglio Nazionale delle Ricerche, Istituto di Farmacologia Traslazionale, UOS Cagliari, Edificio 5, Loc. Piscinamanna, 09010 Pula, CA, Italy*

Corresponding author:

B. Asproni

Dipartimento di Chimica e Farmacia, Università degli Studi di Sassari, Via F. Muroni 23/a, 07100 Sassari, Italy

Tel: +39 079 228749; e-mail: asproni@uniss.it

Abstract

Novel 1,4-dihydropyrazolo[3,4-*a*]pyrrolizine-, 4,5-dihydro-1*H*-pyrazolo[4,3-*g*]indolizine- and 1,4,5,6-tetrahydropyrazolo[3,4-*c*]pyrrolo[1,2-*a*]azepine-3-carboxamide based compounds were designed and synthesized for cannabinoid CB_1 and CB_2 receptor interaction.

All the obtained derivatives exhibited negligeable binding affinity to CB_2 receptors with K_i values that were from 314- to >1μM range. The affinity for CB_1 receptors in most cases was moderate (KiCB_1 = 142-902 nM) with the exception of 7-chloro-1-(2,4-dichlorophenyl)-*N*-(homopiperidin-1-yl)-4,5-dihydropyrazole[4,3-*g*]indolizine-3-carboxamide (**2j**) endowed with a good affinity for CB_1 receptor ($K_i$$CB_1$ = 81nM) and the highest CB_2/CB_1 selectively ratio (>12). Docking studies carried out on such compounds were performed by using the hCB_1 X-ray in complex with the close pirazole analogue AM6538, and discosed specific pattern of interactions related to the tricyclic pyrrolepyrazole scaffolds as CB_1 ligands.

1. Introduction

The cannabinoid CB_1 and CB_2 receptors (CB_1R and CB_2R) belong to the rhodopsin-like family of G-protein-coupled receptors (GPCRs) and are key components of the endocannabinoid system.[1-3] The CB_1R is abundantly expressed in the central nervous system (CNS) but also is present in peripheral tissues, including the lungs, liver, kidneys, and adipocytes.[4] CB_2R is found most abundantly in the periphery, predominantly expressed in cells of the human immune system as spleen, tonsils and thymus,[4] and it is found to a much lesser extent in CNS.[5] CBRs are activated by terpenoid plant constituents, eg., by Δ^9-tetrahydrocannabinol, the major psychoactive component of *Cannabis sativa*.[6] Recent studies have demonstrated that CB_2Rs are involved in numerous diseases.[4,7] Several selective CB_2R agonists exhibited analgesic activity in preclinical models of acute, inflammatory and neuropathic pain.[4,8,9] CB_1 activation mediates analgesia, stimulation of appetite and euphoria, among other effects,[4] and is responsible for the psychotropic effects observed with nonselective cannabinoid ligands.[10] CB_1 receptor antagonists are potential drugs for the therapy of drug and alcohol addiction as well as for the treatment of obesity. In this regard rimonabant (Fig.1) was the first potent CB_1 receptor antagonist[11] approved by European Commission as an anti-obesity agent. However it was soon withdrawn by EMEA for its serious psychiatric disorders including anxiety, depression and suicidal tendency.[12] Within the search for new and safe anti-obesity agents, recent medicinal chemistry approaches are oriented towards the obtainment of new peripherally selective CB_1 antagonists, by designing ligands that do not cross the blood-brain barrier and have low brain penetration.[13-15] The relevance of CBRs as emerging target of pharmacotherapy is documented also by the discovery of peripherally mixed CB_1/CB_2 receptor agonists as antiglaucoma agents.[16]

During the past decade, numerous ligands endowed with high affinities and subtype selectivities for both receptors were synthesized, and within each chemotype the structure activity-relationship (SAR) studies were explored.

The 4-alkyl-5-arylpyrazole skeleton of rimonabant has been modified by us (Fig. 1), giving rise to 1,4-dihydroindeno[1,2-*c*]pyrazole **1A**,[17] 4,5-dihydro-1*H*-benzo[*g*]indazole **1B**[18] and 1,4,5,6-tetrahydrobenzo[6,7]cyclohepta[1,2-*c*]pyrazole-based ligands **1C**[19]. Such tricyclic systems feature a carbamoyl group at position 3 and simple substituents (halogen, methyl, methoxy) on the aryl moieties. These compounds displayed interesting cannabinoid binding affinity and subtype selectivity. In particular, changes to the size and shape of the tricyclic unit

in ligands **1** revealed intriguing effects on the biological activity. Thus, increasing the length of the carbon bridge between C_4 of the pyrazole and the 4-chlorophenyl group from one to three methylene units led to a marked increase in the CB_1 binding affinity and selectivity. Moreover, the presence of a substituent, such as F, Cl, Br, or CH_3, on the phenyl ring of the tricyclic system generally gave an increase in the affinity and selectivity for CB_2 receptors. Compounds **1Aa**, **1Ab**, **1Ba** and **1Ca** are representative of this class of CB ligands. The pharmacological relevance of these compounds emerged from the ability of the CB_2 agonist **1Ab** in alleviating neuropathic pain through functional microglia changes in mice.[20] Furthermore, the analogues CB_1 antagonist compounds NESS06SM and SM-11, featuring the 4,5-dihydrobenzo-oxa-cycloheptapyrazole skeleton could represent useful candidate agents for the treatment of obesity and its metabolic complications.[21]

<<Insert Figure 1>>

Continuing our interest in expanding SAR studies on CBRs,[22] we have undertaken a study to prepare new CB ligands related to both rimonabant and its derivatives **1**. Thus, driven by our understanding of the biological and pharmacological behaviour of the tricyclic pyrazoles, we explored a series of new tricyclic scaffolds incorporating the biologically interesting pyrrole and pyrazole moieties with a central ring that can be modulate in size (Fig. 2 and Tab. 1), namely 1,4-dihydropyrazolo[3,4-*a*]pyrrolizines (**2a-h**), 4,5-dihydro-1*H*-pyrazolo[4,3-*g*]indolizines (**2i-l**), 1,4,5,6-tetrahydropyrazolo[3,4-*c*]pyrrolo[1,2-*a*]azepines (**2m-p**) that varied the carbamoyl moiety with the Cl or CH_3 substituents on the pyrrole moiety. Such bioisosteric benzene/pyrrole replacement might give access to pharmaceutically interesting compounds with modified physical chemical properties, since the introduction of the pyrrole ring renders the tricyclic system more electron-rich. Moreover, it increases the polar surface area and decrease the lipophilicity.

In this paper we report the synthesis of compounds **2a-p** together with preliminary aspects of their affinity and selectivity on CBRs and molecular modelling studies.

<<Insert Figure 2>>

2. Chemistry

The strategy followed for pyrrolcycloalkylpyrazole-based compounds **2** is outlined in Scheme 1 and started with substituted pyrrolcycloalkanones **3-6**.[23] Ketones were first transformed to **7-10** using a Claisen reaction and next condensated with 2,4-dichlorophenylhydrazine to give the tricyclic pyrrolcycloalkylpyrazoles **11-14**. Final elaboration to designed compounds **2a-p** was accomplished by functional interconversion of esters **11-14** *via* acid **15-18** to the amides/hydrazides.

<<Insert Scheme 1>>

3. Results and discussion

Affinities at CB_1 and CB_2 receptors for compounds **2** were assessed by competition for [^{3}H]CP-55,940 binding in mouse whole brain membranes and Chinese hamster ovary (CHO) cell membranes transfected with hCB_2, respectively. The experimental data (IC_{50} values) were converted into K_i values[24] and are shown in Table 1.

In order to investigate how bioisosteric replacement benzene/pyrrole can modify binding profile of the tricyclic scaffold, three series of tricyclic pyrrolpyrazoles **2a-p** structurally correlated to compounds **1Aa, 1Ab, 1Ba and 1Ca**, were synthesized. In general, all the obtained derivatives exhibited negligeable binding affinity to CB_2 receptors with K_i values that were from 314- to >1μM range, while the affinity for CB_1 receptors in most cases was moderate (KiCB_1 = 81- to 902 nM). The 1,4-dihydropyrazolo[3,4-*a*]pyrrolizine compounds **2a-d** with a chlorine atom at C_5 showed moderate binding affinity to CB_1 receptors and values that were from 314- to >1μM range for CB_2 subtype receptor. The highest affinity for both CB receptors was shown by the ligand having the homopiperazine carbamoyl unit. Compound **2b**, the best of this group with a CB_1 receptor affinity of 230 nM and CB_2 receptor affinity of 615 nM was used as reference term for all of the others in terms of presenting SAR studies. Compound **2a**, having a piperazine ring replacement of the homopiperazine ring of the carbamoyl unit, showed much lower affinities for CB_1 receptors as compared to **2b** and no significant affinity for CB_2 receptors (Ki > 1μM). Compound **2c** with a cyclohexyl moiety in the carbamoyl motif exhibited little change in binding affinity between CB_1 and CB_2 receptors however resulting in a 3 to 1.2 fold reduction. Compound **2d**, in which the size and shape of amine unit was markedly changed by introduction of the mirtanyl moiety, had higher CB_2 affinity (2-fold) but lower CB_1 receptor affinity (1,5-fold) as compared to compound **2b**. Changing the chlorine atom on the pyrrole ring of the 1,4-dihydropyrazolopyrrolizine scaffold with a methyl group, compounds **2e-h**, showed some impact

on CB_1 and CB_2 receptor affinity. The mirtanyl derivative **2h** had the highest CB_1 and CB_2 receptor affinity among the four methyl substituted analogues with a CB_1 receptor affinity that is 1,6-fold higher to that of **2b**. CB_2 receptor affinity of **2h** mirrored the ground term **2b**.

The 4,5-dihydro-1*H*-pyrazolo[4,3-*g*]indolizines **2i-l** had higher CB_1 receptor affinities with the only exception of **2l** as compared to **2b**. By contrast, ligands **2i-l** showed no binding preference for CB_2 receptors. Among these derivatives, the homopiperidine substituent analogue, **2j**, had a good affinity for CB_1 receptor (K_iCB_1 = 81nM) to gather with the highest CB_2/CB_1 selectively ratio (>12).

The 1,4,5,6-tetrahydropyrazolo[3,4-*c*]pyrrolo[1,2-*a*]azepines **2m-p** displayed a similar pattern of binding to CB receptor affinities and no significant CB_2 receptor affinities. Among these derivatives, the piperidine substituted analogue, **2m**, had a 1.2-fold higher CB_1 receptor affinity than **2b**.

<<Insert Table 1>>

4. Molecular docking

Nowadays, the rational design and discovery of CB_1 ligands was efficiently driven by deepening computational studies, including homology modelling of the biological target,[25] as well as ligand-based analyses.[26] The recent X-Ray crystallographic structures of the cannabinoid receptor CB_1 became available, providing usuful guidelines for the rational design of novel derivatives (pdb code = 5U09; resolution = 2.6 Å),[27] (pdb code = 5TGZ; resolution = 2.8 Å).[28] These experimental data disclosed the binding mode of the co-crystallized propanamide-based (pdb code = 5U09) and pyrazole-containing (pdb code = 5TGZ) derivatives, shedding light for the design of further series of analogues and/or isosteres.

In this work, we performed docking studies of the newly synthesized compounds, choosing as reference compound the pyrazole ligand (AM6538) co-crystallized in hCB_1 (pdb code = 5TGZ) because of the structural similarity to the derivatives here investigated (Table 1, Supplementary data).

As shown in the following Figures 3-5, AM6538 exhibited one H-bond between the hydrogen atom of the carboxamide group and the side-chain of S383, moving the cyclohexyl substituent

towards I119, F174, A380, M384. The two aromatic centers occupied a deep hydrophobic pocket including I169, L193, V196, F268, W279, L359, W356, M363, L387. In this way, a number of Van der Waals contacts and π–π stacking were detected.

Docking calculations on the newly synthesized molecules (**2a**-**2p**) allowed us to explore the putative binding mode exhibited by the cannabinoid ligands bearing the dihydropyrazolo[3,4-*a*]pyrrolizines (**2a-h**), dihydropyrazolo[4,3-*g*]indolizines (**2i-l**) and the tetrahydropyrazolo[3,4-*c*]pyrrolo[1,2-*a*]azepines (**2m-p**) containing derivatives within the human CB_1 receptor. In particular, the SAR for the three series of compounds has been clarified, when the tryciclic core is coupled with hydrazide or carboxamide moieties as Q group.

Thus, all of them displayed a common positioning, moving the tricyclic core and the phenyl ring toward the two phenyl rings linked to the position 5 and to the position 1 of the pyrazole scaffold in AM6538, in order to gain the same hydrophobic contacts. On the other hand, the hydrazide or the carboxamide moieties exhibited a comparable docking mode, sometimes detecting H-bonds with S383. In particular, the presence of one acid hydrogen atom onto the nitrogen one of the carboxamide (or hydrazide) moiety resulted to be a key-feature for H-bonding S383 side-chain, especially in presence of a bulky hydrophobic group in Q. Among the three series of compounds, the dihydropyrazolo[4,3-*g*]indolizine- and the tetrahydropyrazolo[3,4-*c*]pyrrolo[1,2-*a*]azepine- containing derivatives were well-suited and preferrred to the dihydropyrazolo[3,4-*a*]pyrrolizines. Indeed, compounds **2i**-**2p** moved the tricyclic core much more in proximity of the aforementioned phenyl ring of compound AM6538 (Figure 3, compound **2j** is shown and Figure 4, compound **2n** is shown).

<<Insert Figure 3>>

<<Insert Figure 4>>

Conversely, the dihydropyrazolo[4,3-*g*]indolizines experienced a much more rigid conformation, leading the compound to quite differently accommodate within the human CB_1 binding site (Figure 5, compound **2b** is shown).

<<Insert Figure 5>>

Nevertheless, based on a perspective of the docking results for all the three series of derivatives, adequate CB_1 antagonism could be achieved with the introduction of proper bulky hydrophobic groups in Q. Indeed, this substituent in any case fall within a protein narrow cavity, delimited by I119, F174, A380, M384. Then, flexible hindered tricyclic core proved to be the most suitable in simulate the binding mode of the co-crystallized ligand, making the compound promising in CB_1-targeting.

5. Conclusion

In the present work we synthesized the three series of tricyclic pyrrolepyrazole compounds that differ mainly in the number of atoms bridging the pyrrole nitrogen to pyrazole ring that probably engenders conformational changes in these novel tricyclic scaffolds as those reported for prototypes **1Aa, 1Ab, 1Ba** and **1Ca**. SAR studies conducted on the three series of newly synthesized compounds (**2a-h**, **2i-l** and **2m-p**) revealed for the three series negligeable binding affinity to CB_2 receptors with K_i values that were from 314- to >1μM range. The affinity for CB_1 receptors in most cases was moderate ($K_i CB_1$ = 142-902 nM) with the exception of compound **2j** endowed with a good affinity for CB_1 receptor ($K_i CB_1$ = 81nM) and the highest CB_2/CB_1 selectively ratio (>12). Docking studies carried out on such compounds were performed by using the hCB_1 X-ray in complex with the close pirazole analogue AM6538, and discosed specific pattern of interactions related to the tricyclic pyrrolepyrazole scaffolds as CB_1 ligands. Our preliminary results point out the versatility of the dihydropyrazolo[3,4-*a*]pyrrolizine-, dihydropyrazolo[4,3-*g*]indolizine- and tetrahydropyrazolo[3,4-*c*]pyrrolo[1,2-*a*]azepine architectures to provide novel compounds for CB_1 interaction. The results reported in the present work pave the way for a further design process towards more potent and selective CB_1 ligands.

6. Experimental protocols

6.1. Chemistry

6.1.1 General methods

Melting points were obtained on a Koffler melting point apparatus and are uncorrected. IR spectra were recorded as nujol mulls on NaCl plates with a Jasco FT/IR 460 plus spectrophotometer and are expressed in ν (cm^{-1}). NMR experiments were run on a Bruker AVANCE III Nanobody 400 MHz spectrometer with ^{1}H and ^{13}C being observed at 400 and 100.6 MHz, respectively. Spectra were acquired using $CDCl_3$ as solvent. Chemical shifts for ^{1}H and ^{13}C NMR spectra were reported in δ (ppm) downfield from tetramethylsilane, and coupling constants (*J*) were expressed in Hertz. Multiplicities are recorded as s (singlet), d (doublet), t (triplet), dd (doublet of doublets), m (multiplet). Specific rotation was recorded with a Perkin-Elmer 241 apparatus, using the sodium D line (589 nm), and $CHCl_3$ as solvent. Atmospheric Pressure Ionization Electrospray (API-ES) mass spectra were obtained on an Agilent 1100 series LC/MSD spectrometer. Elemental analyses were performed with a Perkin-Elmer 2400 analyzer, and results were within ±0.40% of the calculated values. TLC was performed on Merck silica gel 60 TLC plates F254 and visualized using UV. Flash chromatography (FC) was performed using Merck silica gel 60 (230–400 mesh ASTM).

Chemical intermediates **3-18** and final compounds **2a**, **2e**, **2i** and **2m** were synthesized according to literature procedure.[23] 1-Aminohomopiperidine, cyclohexylamine and (−)-*cis*-myrtanylamine were purchased by Sigma-Aldrich®.

6.1.2 General procedure for the amidation of 15-18.

1-(3-Dimethylaminopropyl)-3-ethylcarbodiimide (EDC) (1.2 mmol) and 1-hydroxybenzotriazole (BTOH) (1.2 mmol) were added in sequence to a suspension of the appropriate tricyclic acid (1 mmol) in CH_2Cl_2 (15 mL). After 1 h the suspension became a solution and then the appropriate amine (2 mmol) was added and stirring was continued at room temperature overnight. The organic phase was washed with water, dried over anhydrous Na_2SO_4 and concentrated under reduced pressure. The residue was purified by FC.

6.1.2.1 6-Chloro-1-(2,4-dichlorophenyl)-*N*-(homopiperidin-1-yl)-1,4-dihydropyrazole[3,4-*a*]pyrrolizine-3-carboxamide (2b).

Compound **2b** was obtained from **16** and 1-aminohomopiperidine. Yellow solid (0.29 g, 63%); R_f 0.25 (AcOEt/petroleum ether 2/8); mp 167–168 °C; IR 1645 (NH); ^{1}H NMR 7.62 (s, 1H), 7.53 (d, *J* = 8.6 Hz, 1H), 7.42 (d, *J* = 8.6 Hz, 1H), 7.40–7.30 (m, 1H), 6.09 (d, *J* = 3.6 Hz, 1H), 5.92 (d, *J* =

3.8 Hz, 1H), 4.89 (s, 2H), 3.30–3.00 (m, 4H), 1.90–1.50 (m, 8H); ^{13}C NMR 160.1, 141.9, 135.7, 130.8, 129.3, 128.0, 125.3, 124.7, 116.2, 109.3, 100.7, 58.6, 44.0, 27.0, 26.1; API-ES m/z: $[M+H]^+$ calcd for $C_{21}H_{21}Cl_3N_5O$: 464.1, found: 464.1; Anal. ($C_{21}H_{20}Cl_3N_5O$) C, H, N.

6.1.2.2. 6-Chloro-1-(2,4-dichlorophenyl)-*N*-(cyclohexyl-1-yl)-1,4-dihydropyrazole[3,4-*a*]pyrrolizine-3-carboxamide (2c).

Compound **2c** was obtained from **16** and cyclohexylamine. Light brown solid (0.29 g, 65%); R_f 0.61 (AcOEt/petroleum ether 2/8); mp 194–196 °C; IR 1645 (NH); ^{1}H NMR 7.62 (s, 1H), 7.53 (d, J = 8.4 Hz, 1H), 7.42 (d, J = 8.0 Hz, 1H), 6.76 (d, J = 7.6 Hz, 1H), 6.08 (d, J = 2.8 Hz, 1H), 5.92 (d, J = 2.8 Hz, 1H), 4.91 (s, 2H), 4.08–3.78 (m, 1H), 2.15–1.88 (m, 2H), 1.88–1.71 (m, 2H), 1.71–1.50 (m, 1H), 1.50–1.34 (m, 2H), 1.36–1.10 (m, 3H); ^{13}C NMR 160.2, 141.9, 135.9, 130.8, 129.1, 128.3, 125.3, 124.7, 116.1, 109.4, 100.7, 48.3, 45.6, 33.3, 25.7, 25.1; API-ES m/z: $[M+H]^+$ calcd for $C_{21}H_{20}Cl_3N_4O$: 449.1, found: 449.2; Anal. ($C_{21}H_{19}Cl_3N_4O$) C, H, N.

6.1.2.3. 6-Chloro-1-(2,4-dichlorophenyl)-*N*-(*cis*-myrtanyl-1-yl)-1,4-dihydropyrazole[3,4-*a*]pyrrolizine-3-carboxamide (2d).

Compound **2d** was obtained from **16** and (−)-*cis*-myrtanylamine. Light brown solid (0.28 g, 55%); mp 250-253 °C; R_f 0.55 (AcOEt/petroleum ether 2/8); IR 1645 (NH); ^{1}H NMR 7.72 (s, 1H), 7.53 (d, J = 8.8 Hz, 1H), 7.43 (d, J = 8.8 Hz, 1H), 7.00–6.85 (m, 1H), 6.08 (d, J = 4.0 Hz, 1H), 5.92 (d, J = 4.0 Hz, 1H), 4.91 (s, 2H), 3.46–3.29 (m, 2H), 2.42–2.11 (m, 2H), 2.00–1.40 (m, 6H), 1.20 (s, 3H), 1.08 (s, 3H), 0.90 (d, J = 9.6 Hz, 1H); ^{13}C NMR 160.3, 142.5, 141.6, 135.7, 130.8, 130.2, 129.1, 128.7, 128.3, 125.0, 124.7, 116.1, 109.3, 100.9, 44.9, 44.8, 44.1, 41.7, 41.5, 38.9, 33.6, 28.0, 26.1, 23.4, 20.3; $[\alpha]_D$ -2.41 (*c* 0.1678, $CHCl_3$); API-ES m/z: $[M+H]^+$ calcd for $C_{25}H_{26}Cl_3N_4O$: 503.1, found: 503.2; Anal. ($C_{25}H_{25}Cl_3N_4O$) C, H, N.

6.1.2.4. 6-Methyl-1-(2,4-dichlorophenyl)-*N*-(homopiperidin-1-yl)-1,4-dihydropyrazole[3,4-*a*]pyrrolizine-3-carboxamide (2f).

Compound **2f** was obtained from **15** and 1-aminohomopiperidine. White solid (0.20 g, 45%). R_f 0.25 (AcOEt/petroleum ether 2/8); mp 154–155 °C; IR 1648 (NH); ^{1}H NMR 8.26 (s, 1H), 7.61 (s, 1H), 7.52 (d, J = 8.4 Hz, 1H), 7.41 (d, J = 8.1 Hz, 1H), 5.98–5.91 (m, 1H), 5.92–5.81 (m, 1H), 4.82 (s, 2H), 3.35–3.03 (m, 4H), 2.27 (s, 3H), 1.87–1.77 (m, 4H), 1.73–1.61 (m, 4H); ^{13}C NMR 158.9, 145.4, 135.7, 135.6, 130.6, 129.3, 128.8, 128.1, 125.1, 124.9, 124.8, 109.6, 99.9, 58.5, 44.4, 26.9, 26.0, 11.9; API-ES m/z: $[M+H]^+$ calcd for $C_{22}H_{24}Cl_2N_5O$: 444.1, found: 444.2; Anal. ($C_{22}H_{23}Cl_2N_5O$) C, H, N.

6.1.2.5. 6-Methyl-1-(2,4-dichlorophenyl)-*N*-(cyclohexyl-1-yl)-1,4-dihydropyrazole[3,4-*a*]pyrrolizine-3-carboxamide (2g).

Compound **2g** was obtained from **15** and cyclohexylamine. White solid (0.21 g, 49%). R_f 0.60 (AcOEt/petroleum ether 2/8); mp 130–133 °C; IR 1653 (NH); ^{1}H NMR 7.61 (d, *J* = 1.6 Hz, 1H), 7.53 (d, *J* = 8.6 Hz, 1H), 7.41 (dd, *J* = 8.6, 1.6 Hz, 1H), 6.80 (d, *J* = 8.0 Hz, 1H), 5.94 (d, *J* = 3.0 Hz, 1H), 5.88 (d, *J* = 3.0 Hz, 1H), 4.83 (s, 2H), 4.04–3.84 (m, 1H), 2.27 (s, 3H), 2.07–1.97 (m, 2H), 1.80–1.72 (m, 2H), 1.68–1.58 (m, 1H), 1.50–1.35 (m, 2H), 1.35–1.03 (m, 3H); ^{13}C NMR 160.5, 145.5, 142.0, 135.9, 135.7, 130.8, 130.7, 129.4, 129.0, 128.2, 125.1, 125.0, 109.6, 99.9, 48.3, 44.6, 33.3, 25.7, 25.1, 12.0; API-ES m/z: $[M+H]^+$ calcd for $C_{22}H_{23}Cl_2N_4O$: 429.1, found: 429.0; Anal. ($C_{22}H_{22}Cl_2N_4O$) C, H, N.

6.1.2.6. 6-Methyl-1-(2,4-dichlorophenyl)-*N*-(*cis*-myrtanyl-1-yl)-1,4-dihydropyrazole[3,4-*a*]pyrrolizine-3-carboxamide (2h).

Compound **2h** was obtained from **15** and (−)-*cis*-myrtanylamine . White solid (0.17 g, 35%). R_f 0.62 (AcOEt/petroleum ether 2/8); mp 178–179 °C; IR 1651 (NH). ^{1}H NMR 7.62 (d, *J* = 2.0 Hz, 1H), 7.53 (d, *J* = 8.6 Hz, 1H), 7.41 (dd, *J* = 8.6, 2.0 Hz, 1H), 6.98 (d, *J* = 6.0 Hz, 1H), 5.94 (d, *J* = 3.6 Hz, 1H), 5.88 (d, *J* = 3.6 Hz, 1H), 4.84 (s, 2H), 3.56–3.33 (m, 2H), 2.40–2.29 (m, 2H), 2.27 (s, 3H), 2.03–1.96 (m, 2H), 1.96–1.81 (m, 3H), 1.64–1.51 (m, 1H), 1.21 (s, 3H), 1.09 (s, 3H), 0.91 (d, *J* = 9.6 Hz, 1H). ^{13}C NMR 161.5, 145.6, 141.8, 135.9, 135.7, 130.9, 130.8, 129.4, 128.9, 128.2, 125.2, 124.9, 109.6, 99.9, 44.9, 44.7, 43.9, 41.7, 41.5, 38.9, 33.4, 28.1, 26.2, 23.4, 20.0, 12.0; $[\alpha]_D$ -3.08 (*c* 0.2048, $CHCl_3$); API-ES m/z: $[M+H]^+$ calcd for $C_{26}H_{29}Cl_2N_4O$: 483.2, found: 483.3; Anal. ($C_{26}H_{28}Cl_2N_4O$) C, H, N.

6.1.2.7. 7-Chloro-1-(2,4-dichlorophenyl)-*N*-(homopiperidin-1-yl)-4,5-dihydropyrazole[4,3-*g*]indolizine-3-carboxamide (2j).

Compound **2j** was obtained from **17** and 1-aminohomopiperidine. White solid (0.17 g, 36%); R_f 0.28 (AcOEt/petroleum ether 2/8); mp 150–152 °C; IR 1645 (NH); ^{1}H NMR 8.01 (s, 1H), 7.63 (s, 1H), 7.46–7.38 (m, 2H), 5.93 (d, *J* = 4.2 Hz, 1H,), 5.41 (d, *J* = 3.8 Hz, 1H), 4.10 (t, *J* = 6.8 Hz, 2H), 3.39 (t, *J* = 6.8 Hz, 2H), 3.14 (t, *J* = 5.6 Hz, 4H), 1.80–1.45 (m, 8H); ^{13}C NMR 161.5, 143.6, 137.1, 136.8, 136.2, 133.9, 130.7, 130.6, 128.3, 120.7, 119.1, 112.7, 107.2, 104.4, 58.5, 42.3, 26.9, 26.0, 20.7; API-ES m/z: $[M+H]^+$ calcd for $C_{22}H_{23}Cl_3N_5O$: 478.1, found: 478.0; Anal. ($C_{22}H_{22}Cl_3N_5O$) C, H, N.

6.1.2.8. 7-Chloro-1-(2,4-dichlorophenyl)-*N*-(cyclohexyl-1-yl)-4,5-dihydropyrazole[4,3-*g*]indolizine-3-carboxamide (2k).

Compound **2k** was obtained from **17** and cyclohexylamine. Light brown solid (0.18 g, 40%). R_f 0.55 (AcOEt/petroleum ether 2/8); mp 190–192 °C; IR 1650 (NH); ^{1}H NMR 7.62 (s, 1H), 7.44 (s, 2H), 6.85–6.58 (m, 1H), 5.94 (d, *J* = 4.0 Hz, 1H), 5.40 (d, *J* = 4.0 Hz, 1H), 4.10 (d, *J* = 6.8 Hz, 2H), 4.01–3.84 (m, 1H), 3.40 (d, *J* = 6.8 Hz, 2H), 2.01 (d, *J* = 12.0 Hz, 2H), 1.82–1.66 (m, 2H), 1.68–1.60 (m, 1H), 1.46–1.12 (m, 5H); ^{13}C NMR 161.5, 143.6, 137.0, 136.9, 136.0, 133.8, 130.7, 130.5, 128.3, 120.7, 119.0, 112.7, 107.2, 104.4, 48.2, 42.3, 33.3, 25.7, 25.1, 20.9; API-ES m/z: $[M+H]^+$ calcd for $C_{22}H_{22}Cl_3N_4O$: 463.1, found: 463.2; Anal; ($C_{22}H_{21}Cl_3N_4O$) C, H, N.

6.1.2.9. 7-Chloro-1-(2,4-dichlorophenyl)-*N*-(*cis*-myrtanyl-1-yl)-4,5-dihydropyrazole[4,3-*g*]indolizine-3-carboxamide (2l).

Compound **2l** was obtained from **17** and (−)-*cis*-myrtanylamine. Light brown solid (0.31 g, 61%); R_f 0.60 (AcOEt/petroleum ether 2/8); mp 192-193 °C; IR 1645 (NH); ^{1}H NMR 7.63 (s, 1H), 7.45 (s, 2H), 7.00–6.80 (m, 1H), 5.95 (d, *J* = 3.2 Hz, 1H), 5.41 (d, *J* = 3.0 Hz, 1H), 4.10 (t, *J* = 7.0 Hz, 2H), 3.40 (t, *J* = 7.0, 2H), 3.50–3.31 (m, 2H), 2.41–2.23(m, 2H), 2.01–1.84 (m, 5H), 1.73–1.52 (m, 1H), 1.20 (m, 3H), 1.07 (s, 3H), 1.00–0.80 (m, 1H); ^{13}C NMR 161.5, 143.6, 137.0, 136.9, 136.0, 133.8, 130.7, 130.5, 128.3, 120.7, 119.0, 112.7, 107.2, 104.4, 44.9, 44.5, 43.9, 41.5, 41.1, 38.6, 33.1, 28.7, 26.2, 23.4, 20.1; $[\alpha]_D$ -1.86 (*c* 0.20, $CHCl_3$); API-ES m/z: $[M+H]^+$ calcd for $C_{26}H_{28}Cl_3N_4O$: 517.1, found: 517.2; Anal. ($C_{26}H_{27}Cl_3N_4O$): C, H, N.

6.1.2.10. 8-Chloro-1-(2,4-dichlorophenyl)-*N*-(homopiperidin-1-yl)-1,4,5,6-tetrahydropyrazole[3,4-*c*]pyrrole [1,2-*a*]azepine-3-carboxamide (2n).

Compound **2n** was obtained from **18** and homopiperidine. Pink solid (0.20 g, 40%). R_f 0.21 (AcOEt/petroleum ether 2/8); mp 160-162 °C; IR 1645 (NH). ^{1}H NMR 8.04 (s, 1H), 7.54 (s, 1H), 7.46–7.35 (m, 2H), 5.89 (d, *J* = 4.0 Hz, 1H,), 5.33 (d, *J* = 3.8 Hz, 1H,), 4.20–4.05 (m, 2H), 3.40–3.20 (m, 3H), 3.19–3.05 (m, 3H), 2.31–2.22 (m, 2H), 1.82–1.54 (m, 8H). ^{13}C NMR (101 MHz, $CDCl_3$) 163.2, 146.5, 136.2, 135.9, 133.9, 133.6, 130.7, 130.4, 128.2, 121.8, 117.9, 116.4, 108.4, 106.9, 58.3, 44.7, 26.9, 26.2, 23.9; API-ES m/z: $[M+H]^+$ calcd for $C_{23}H_{25}Cl_3N_5O$: 492.1, found: 492.2; Anal. ($C_{23}H_{24}Cl_3N_5O$) C, H, N.

6.1.2.11. 8-Chloro-1-(2,4-dichlorophenyl)-*N*-(cyclohexyl-1-yl)-1,4,5,6-tetrahydropyrazole[3,4-*c*]pyrrole [1,2-*a*]azepine-3-carboxamide (2o).

Compound **2o** was obtained from **18** and cyclohexylamine. Pink solid (0.20 g, 42%); R_f 0.21 (AcOEt/petroleum ether 1/1); mp 150–152 °C; IR 1645 (NH). ^{1}H NMR 7.53 (s, 1H), 7.41 (s, 2H), 6.83 (d, *J* = 7.6 Hz, 1H), 5.89 (d, *J* = 2.6 Hz, 1H), 5.33 (d, *J* = 2.4 Hz, 1H), 4.20–4.05 (m, 2H), 4.00–3.83 (m, 1H), 3.42–3.24 (m, 2H), 2.24–2.10 (m, 2H), 2.10–1.88 (m, 2H), 1.87–1.50 (m, 4H), 1.44–1.36 (m, 4H); ^{13}C NMR: 163.2, 146.5, 136.2, 135.9, 133.7, 133.6, 130.7, 130.4, 128.2, 121.8, 117.9, 116.4, 108.4, 106.9, 48.3, 44.7, 44.6, 33.3, 26.9, 25.7, 24.0, 25.1; API-ES m/z: $[M+H]^+$ calcd for $C_{23}H_{24}Cl_3N_4O$: 477.1, found: 477.0; Anal. ($C_{23}H_{23}Cl_3N_4O$): C, H, N.

6.1.2.12. 8-Chloro-1-(2,4-dichlorophenyl)-*N*-(*cis*-myrtanyl-1-yl)-1,4,5,6-tetrahydropyrazole[3,4-*c*]pyrrole [1,2-*a*]azepine-3-carboxamide (2p).

Compound **2p** was obtained from **18** and (−)-*cis*-myrtanylamine. Light brown solid (0.16 g, 30%). R_f 0.68 (AcOEt/petroleum ether 2/8); mp 154–155 °C; IR 1645 (NH). ^{1}H NMR 7.53 (s, 1H), 7.42–7.30 (m, 2H), 7.10–6.90 (m, 1H), 5.89 (s, 1H), 5.34 (s, 1H), 4.23–4.05 (m, 2H), 3.44–3.23 (m, 2H), 3.10–3.02 (m, 2H), 2.41–2.10 (m, 4H), 2.00–1.88 (m, 2H), 1.88–1.76 (m, 3H), 1.60–1.48 (m, 1H), 1.19 (s, 3H), 1.07 (s, 3H), 0.80–1.00 (m, 1H). ^{13}C NMR 163.1, 146.5, 136.4, 136.1, 133.8, 133.6, 130.7, 130.5, 128.5, 121.8, 118.0, 116.4, 108.3, 107.1, 44.7, 44.2, 44.1, 42.0, 41.4, 38.8, 33.4, 28.2, 26.1, 26.0, 24.0, 23.5, 20.3; $[\alpha]_D$ -2.10 (*c* 0.2017, $CHCl_3$). API-ES m/z: $[M+H]^+$ calcd for $C_{27}H_{30}Cl_3N_4O$: 531.1, found: 531.2; Anal. ($C_{27}H_{29}Cl_3N_4O$) C, H, N.

6.2. Biological assays

6.2.1. Radioreceptor binding assays

6.2.1.1. General procedures binding experiments.

Affinities at CB_1 and CB_2 receptors for **2a-p** were assessed by competition for [^{3}H]CP-55,940 binding in mouse whole brain membranes and Chinese hamster ovary (CHO) cell membranes transfected with hCB_2, respectively.[29]

6.2.1.2. Mouse Brain Membranes.[30]

Whole mouse brains from four adult male MF1 mice were suspended in centrifugation buffer (320 mM sucrose, 2 mM Tris•HCl, 2 mM Tris base, 2 mM EDTA, 5 mM $MgCl_2$ at pH 7.4) and the tissue homogenized with an Ultra-Turrex homogenizer. Tissue homogenates were centrifuged at 1600g for 10 min and the resulting supernatant collected. The pellet was resuspended in centrifugation buffer, centrifuged as before and the supernatant collected. Supernatants were combined before undergoing further centrifugation at 28,000g for 20 min. The supernatant was discarded and the pellet resuspended in 20 ml of buffer A (50 mM Tris•HCl, 50 mM Tris base, 2

mM EDTA, 5 mM $MgCl_2$ at pH 7.0) and incubated at 37 °C for 10 min. Following the incubation, the suspension was centrifuged for 20 min at 23,000g. After resuspending the pellet in another 20 ml of buffer A, the suspension was incubated for 40 min at room temperature before a final centrifugation for 15 min at 11,000g. The final pellet was resuspended in 2 ml of buffer B (50 mM Tris•HCl, 50 mM Tris base, 1 mM EDTA, 3 mM MgCl2 at pH 7.4) to give a protein concentration of 1 mg/ml and stored at 80 °C. All centrifugation procedures were carried out at 4 °C.

6.2.1.3. CHO cell membranes.[29]

CHO cells stably transfected with cDNA encoding human cannabinoid CB_2 receptors (Bmax = 72.6 pmol/mg protein) were maintained at 37 °C and 5% CO_2 in Dulbecco's Modified Eagles's medium (DMEM) nutrient mixture F-12 HAM supplemented with 10% Foetal Bovine Serum (FBS), 3 ml penicillin-streptomycin and 4 ml G-418. These CHO hCB_2 cells were passed twice a week using a nonenzymatic cell dissociation solution (5 ml EDTA). The hCB_2 transfected cells were removed from flasks by scraping and then frozen as a pellet at 20 °C until required. Before use in a radioligand-binding assay, cells were defrosted, diluted in 50 mM Tris-binding buffer (see radioligand displacement assay), and homogenized with a 1 ml hand-held homogenizer. Protein assays were performed using a Bio-Rad Dc kit.

6.2.1.4. Radioligand displacement assay.[29]

Binding experiments were carried out with [^{3}H]CP-55,940, Tris-binding buffer (50 mM Tris•HCl, 50 mM Tris base; 0.1% BSA, pH 7.4), total assay volume 500 ml, using the filtration procedure described previously by Ross et al.[19] Binding was initiated by the addition of mouse brain (CB_1 assay) or CHO cells (CB_2 assay) membranes (50 μg protein per tube). All assays were performed at 37 °C for 60 min before termination by addition of ice-cold Tris-binding buffer and vacuum filtration using a 12-well sampling manifold (Cell Harvester; Brandel) and Whatman GF/B glass-fibre filters that had been soaked in wash buffer at 4 °C for 24 h. Each reaction tube was washed five times with the wash buffer. The filters were oven-dried for 60 min and then placed in 5 ml of scintillation fluid. Radioactivity was quantified by liquid scintillation spectrometry. *Specific binding* was defined as the difference between the binding that occurred in the presence and absence of 1 μM unlabelled CP-55,940. The concentration of [^{3}H]CP-55,940 used in our displacement assays was 0.7 nM. Each unlabelled cannabinoid tested was stored as a stock solution of 10 mM in DMSO, the vehicle concentration in all assay tubes being 0.1% DMSO. Protein assays were performed using a Bio-Rad Dc kit. The binding parameters for [^{3}H]CP-55,940, determined by fitting data from saturation-binding experiments to a one-site saturation

plot using GraphPad Prism, were 2336 fmol/mg protein (Bmax) and 2.31 nM (Kd) in mouse brain membranes, and 72,570 fmol/mg protein (Bmax) and 4.3 nM (Kd) in hCB_2-transfected cells.

6.3. Molecular docking

6.3.1. Ligand Preparation and Docking studies

All the compounds were built, parameterized (Gasteiger-Huckel method) and energy minimized within MOE using MMFF94 forcefield.[31]

Docking calculations within the X-ray structure of the cannabinoid receptor CB_1 (pdb code = 5TGZ; resolution = 2.8 Å)[28] were performed using the LeadIT 2.1.8 software suite.[32] This tool includes the FlexX scoring algorithm, which is based on calculation of the binding free energy by means of Gibbs-Helmholtz equation.[33] The software detects the binding site defining a radius of 10 Å far from the co-crystallized ligand, in order to set up a spherical search space for the docking approach.

The standard setting as docking strategy was followed, choosing the so-called Hybrid Approach (enthalpy and entropy criteria), the related scoring function evaluation is described in the literature.[34] The derived docking poses were prioritized taking into account the score values of the lowest energy pose of the compounds docked to the protein structure. All ligands were further refined and rescored by assessment with the algorithm HYDE, included in the LeadIT 2.1.8 software. The HYDE module considers dehydration enthalpy and hydrogen bonding.[35]

Then, the stability of the selected protein-ligand complexes was assessed using a short ~1 ps run of molecular dynamics (MD) at constant temperature, followed by an all-atom energy minimization (LowModeMD implemented in MOE software). This kind of module allowed to perform an exhaustive conformational analysis of the ligand-receptor binding site subset, as we previously reported about other case studies. [22e,36]

Conflict of interest

None of the authors have conflict of interest to declare.

Appendix A. Supplementary data

Supplementary data related to this article can be found at…

References

1. Reggio, P. H. *Curr. Med. Chem.* **2010**, *17*, 1468.
2. Di Marzo, V.; Bifulco, M.; De Petrocellis, L. *Nat. Rev. Drug Discov.* **2004**, *3*, 771.
3. Boyd, S. T. **2006**, *26*, 218S.
4. Pacher, P.; Batkai, S.; Kunos, G. *Pharmacol. Rev*. **2006**, *58*, 389.
5. Gong, J.-P.; Onaivi, E. S.; Ishiguro, H.; Liu, Q.-R.; Tagliaferro, P. A.; Brusco, A.; Uhl, G. R. *Brain Res*. **2006**, *1071*, 10.
6. Gaoni, Y.; Mechoulam, R. *J. Am. Chem. Soc.* **1964**, *86*,1646.
7. (a) Han, S.; Thatte, J.; Buzard, D. J.; Jones, R. M. *J. Med. Chem*. **2013**, *56*, 8224. (b) Tabrizi, M. A.; Baraldi, P. G.; Borea, P. A.; Varani, K. *Chem. Rev*. **2016**, *116,* 519.
8. (a) Murineddu, G.; Asproni, B.; Pinna, G. A. *Rec. Pat. CNS Drug Discovery*, **2012**, *7*, 4. (b) Murineddu, G.; Deligia, F.; Dore, A.; Pinna, G.; Asproni, B.; Pinna, G. A. *Rec. Pat. CNS Drug Discovery*, **2013**, *8*, 42.
9. Racz, I.; Nadal, X.; Alferink, J.; Banos, J. E.; Rehnelt, J.; Martin, M.; Pintado, B.; Gutierrez-Adan, A.; Sanguino, E.; Manzanares, J.; Zimmer, A.; Maldonado, R. *J. Neurosci*. **2008**, *28*, 12125.
10. Pertwee, R. G.; Howlett, A. C.; Abood, M. E.; Alexander, S. P. H.; Di Marzo, V.; Elphick, M. R.; Greasley, P. J.; Hansen, H. S.; Kunos, G.; Mackie, K.; Mechoulam, R.; Ross, R. A. *Pharmacol. Rev.* **2010**, *62*, 588.
11. (a) Rinaldi-Carmona, M.; Barth, F.; Hkaulme, M.; Shire, D.; Calandra, B.; Congy, C.; Martinez, S.; Maruani, J.; Neliat, G.; Caput, D.; Ferrara, P.; Soubrie, P.; Breliere, J. C.; Le Fur, G. *FEBS Letters* **1994**, *350*, 240. (b) Barth, F.; Rinaldi-Carmona, M. *Curr. Med. Chem*. **1999**, *6*, 745.
12. Jones, D. *Nat. Rev. Drug Discov.*, **2008**, *7*, 961.
13. Sharma, M. K.; Murumkar, P. R.; Kanhed, A. M.; Giridhar, R.; Yadav, M. R. *Europ. J. Med. Chem*. **2014**, *79* 298.

14. Fulp, A.; Bortoff, K.; Zhang, Y.; Snyder, R.; Fennell, T.; J. A.; Marusich, J. A.; Wiley, J. L.; Seltzman, H.; Maitra, R. *J. Med. Chem.* **2013**, *56*, 8066.

15. Röver, S.; Andjelkovic, M.; Beńardeau, A.; Chaput, E.; Guba, W.; Hebeisen, P.; Mohr, S.; Nettekoven, M.; Obst, U.; Richter, W. F.; Ullmer, C.; Waldmeier, P.; Wright, M. B. *J. Med. Chem*. **2013**, *56*, 9874.

16. Mainolfi, N.; Powers, J.; Amin, J.; Long, D.; Lee, W.; McLaughlin, M. E.; B. Jaffee, B.; Brain, C.; Elliott, J.; Sivak, J. M. *J. Med. Chem*. **2013**, *56*, 5464.

17. Mussinu, J.-M.; Ruiu, S.; Mulè, A. C.; Pau, A.; Carai, M. A. M.; Loriga, G.; Murineddu, G.; Pinna, G. A. *Bioorg. Med. Chem*. **2003**, *11*, 251.

18. Murineddu, G.; Ruiu, S.; Mussinu, J.-M.; Loriga, G.; Grella, G. E.; Carai, M. A. M.; Lazzari, P.; Pani, L.; Pinna, G. A. *Bioorg. Med. Chem*. **2005**, *13*, 3309.

19. Lazzari, P.; Distinto, R.; Manca, I.; Baillie, G.; Murineddu, G.; Pira, M.; Falzoi, M.; Sani, M.; Morales, P.; Ross, R.; Zanda, M.; Jagerovic, N.; Pinna, G. A. *Europ. J. Med. Chem*. **2016**, *121*, 194.

20. Luongo, L.; Palazzo, E.; Tambaro, S.; Giordano, C.; Gatta, L.; Scafuro, M. A.; Rossi, F.; Lazzari, P.; Pani, L.; de Novellis, V.; Malcangio, M.; Maione, S. *Neurobiology of Disease*, **2010**, *37*.

21. (a) Mastinu, A.; Pira, M.; Pinna, G. A.; Pisu, C.; Casu, M. A.; Reali, R.; Marcello, S.; Murineddu, G.; Lazzari. P. *Pharmacol. Res.* **2013**, *74*, 94. (b) Fois, G. R.; Fattore, L.; Murineddu, G.; Salis, A.; Pintore, G.; Asproni, B.; Pinna, G. A.; Diana, M. *Pharmacol. Res.* **2016**, *113*, 108.

22. (a) Lazzari, P.; Pau, A.; Tambaro, S.; Asproni, B.; Ruiu, S.; Pinna, G.; Mastinu, A.; Curzu, M. M.; Reali, R.; Bottazzi, M. E. H.; Pinna, G. A.; Murineddu, G. *Central Nervous System Agents in Medicinal Chemistry*, **2012**, *12*, 254. (b) Murineddu, G.; Asproni, B.; Ruiu, S.; Deligia, F.; Falzoi, M.; Pau, A.; Thomas, B. F. Y.; Zhang, Y.; Pinna, G. A.; Pani, L.; Lazzari, P. *The Open Medicinal Chemistry Journal,* **2012***, 6,* 1. (c) Pinna, G.; Loriga, G.; Lazzari, P.; Ruiu, S.; Falzoi M.; Frau, S.; Pau, A.; Murineddu, G.; Asproni, B.; Pinna, G. A. *Eur. J. Med. Chem*. **2014**, *82*, 281. (d) Pinna, G.; Curzu, M. M.; Dore, A.; Lazzari, P.; Ruiu, S.; Pau, A.; Murineddu, G.; Pinna, G. A. *Eur. J. Med. Chem*. 2014, *85*, 747. (e) Deiana, V.; Gomez-Cañas, M.; Pazos, M. R.; Fernàndez-Ruiz, J.; Ruiz, Asproni, B.; Cichero, E.; Fossa, P.; Muñoz, E.; Deligia, F.; Murineddu, G.; García-Arencibia, M.; Pinna, G. A. *Europ. J. Med. Chem*. **2016**, *112*, 66. (f) Dore, A.; Asproni, B.; Scampuddu, A.; Gessi, S.; Murineddu, G.; Cichero, E.; Fossa, P.; Merighi, S.; Bencivenni, S.; Pinna, G. A. *Bioorg. Med. Chem.* **2016**, *24*, 5291. (g) Ragusa, G.; Gomez-Cañas, M.; Morales, P.; Rodríguez-Cueto, C.; Pazos, M. R.; Asproni, B.;

Cichero, E.; Fossa, P.; Pinna, G. A.; Jagerovic, N.; Fernàndez-Ruiz, J.; Murineddu, G. *Europ. J. Med. Chem*. **2017**, *127*, 398.

23. Pinna, G.; Pinna, G. A.; Chelucci, G.; Baldino, S. *Synthesis*, **2012**, *44*, 2798.

24. Cheng, Y.; Prusoff, W. H. *Biochem. Pharmacol.* **1973**, *22*, 3099.

25. (a) Tuccinardi, T.; Ferrarini, P. L.; Manera, C.; Ortore, G.; Saccomanni, G.; Martinelli, A.; *J. Med. Chem.* **2006**, *49*, 984. (b) Menozzi, G.; Fossa, P.; Cichero, E.; Spallarossa, A.; Ranise, A.; Mosti, L. *Eur. J. Med. Chem.* **2008**, *43*, 2627.

26. Cichero, E.; Menozzi, G.; Spallarossa, A.; Mosti, L.; Fossa, P. *J. Mol. Model*. **2008**, *14*, 1131.

27. Shao, Z.; Yin, J.; Chapman, K.; Grzemska, M.; Clark, L.; Wang, J.; Rosenbaum, D. M.; *Nature*, **2016**, *540*, 602.

28. Hua, T.; Vemuri, K.; Pu, M.; Qu, L.; Han, G. W.; Wu, Y., Zhao, S.; Shui, W.; Li, S.; Korde, A.; Laprairie, R. B.; Stahl, E. L.; Ho, J.−H.; Zvonok, N.; Zhou, H.; Kufareva, I.; Wu, B.; Zhao, Q.; Hanson, M. A.; Bohn, L. M.; Makriyannis, A.; Stevens, R. C.; Liu, Z.−J. *Cell*, **2016**, *167*, 750.

29. (a) Ross, R. A.; Brockie, H. C.; Stevenson, L. A.; Murphy, V. L.; Templeton, F.; Makriyannis, A.; Pertwee, R. G. *Br. J. Pharmacol*. **1999**, *126*, 665. (b) Thomas, A.; Stevenson, L. A.; Wease, K. N.; Price, M. R.; Ballie, G.; Ross, R. A.; Pertwee, R. G. *Br. J. Pharmacol*. **2005**, *146*, 917.

30. Lazzari, P.; Loriga, G.; Manca, I.; Pinna, G. A.; Pani, L. U.S. Patent Application US 2010/0215741, Aug. 26, **2010**.

31. MOE: Chemical Computing Group Inc . Montreal. H3A 2R7 Canada. http://www.chemcomp.com.

32. www.biosolveit.com.

33. (a) Böhm, H.-J. *J. Comput. Aided Mol. Des.* **1992**, *6*, 61. (b) . Böhm, H.-J. *J. Comput. Aided Mol. Des.* **1994**, *8*, 243. (c) Rarey, M.; Kramer, B.; Lengauer, T.; Klebe, G. *J. Mol. Biol*. **1996**, *261*, 470.

34. Bichmann, L.; Wang, Y.-T.; Fischer, W. B. *Comput. Biol. Chem*. **2014**, *53*, 308.

35. (a) Reulecke, I.; Lange, G.; Albrecht, J.; Klein, R.; Rarey, M. *Chem. Med. Chem*. **2008**, *3*, 885. (b) Schneider, N.; Hindle, S.; Lange, G.; Klein, R.; Albrecht, J.; Briem, H.; Beyer, K.; Claußen, H.; Gastreich, M.; Lemmen, C.; Rarey, M. *J. Comput. Aided Mol. Des*. **2012**, *26*, 701.

36. Fossa, P.; Cichero, E. *Bioorg. Med. Chem*., **2015**, *23,* 3215.

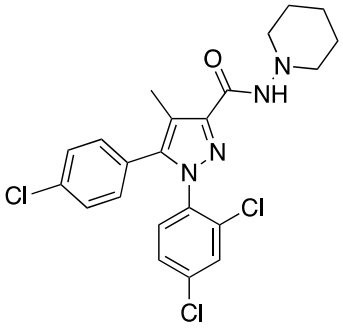

rimonabant

K_iCB_1 = 1.8 nM
K_iCB_2 = 514 nM
CB_1 selectivity = K_iCB_2/K_iCB_1 = 285.5

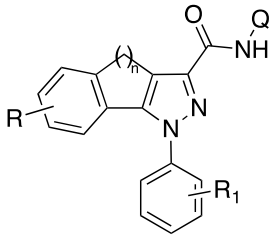

1

n = 1(A); n = 2(B); n = 3(C)

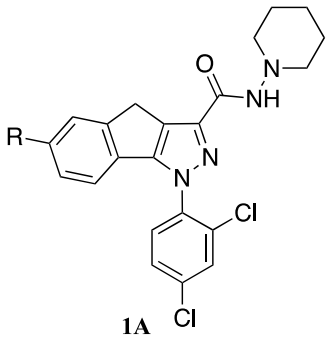

1A

1Aa: R = Cl K_iCB_1 = 2050 nM
K_iCB_2 = 0.34 nM
CB_1 selectivity = K_iCB_2/K_iCB_1 = 0.000166

1Ab: R = CH_3 K_iCB_1 = 363 nM
K_iCB_2 = 0.037 nM
CB_1 selectivity K_iCB_2/K_iCB_1 = 0.000102

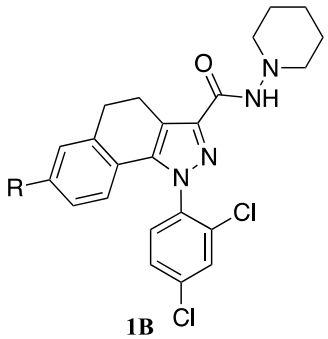

1B

1Ba: R = Cl K_iCB_1 = 14.8 nM
K_iCB_2 = 227 nM
CB_1 selectivity K_iCB_2/K_iCB_1 = 15.3

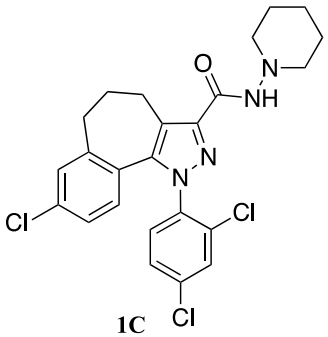

1C

1Ca: R = Cl K_iCB_1 = 4.2 nM
K_iCB_2 = 55.7 nM
CB_1 selectivity K_iCB_2/K_iCB_1 = 13.3

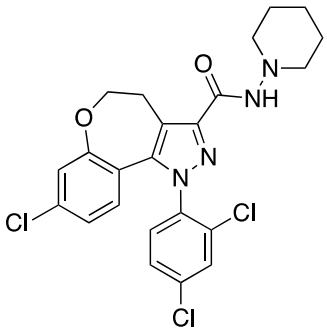

NESS06SM

K_iCB_1 = 10.2 nM
K_iCB_2 = > 5000 nM
CB_1 selectivity K_iCB_2/K_iCB_1 = > 490.2

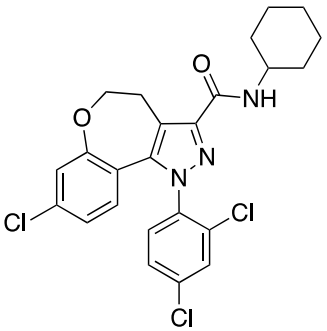

SM-11

K_iCB_1 = 40.0 nM
K_iCB_2 = > 3725 nM
CB_1 selectivity K_iCB_2/K_iCB_1 = > 93.1

Figure 1. Chemical structures of CBRs ligands.

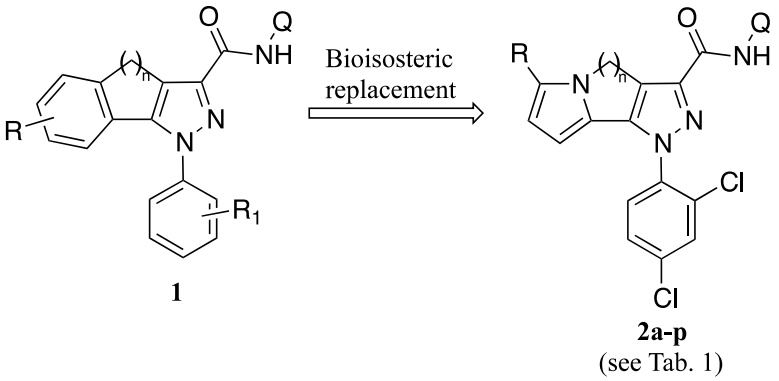

1 **2a-p**
(see Tab. 1)

Figure 2. Design of CBR ligands by bioisosteric replacement benzene/pyrrole.

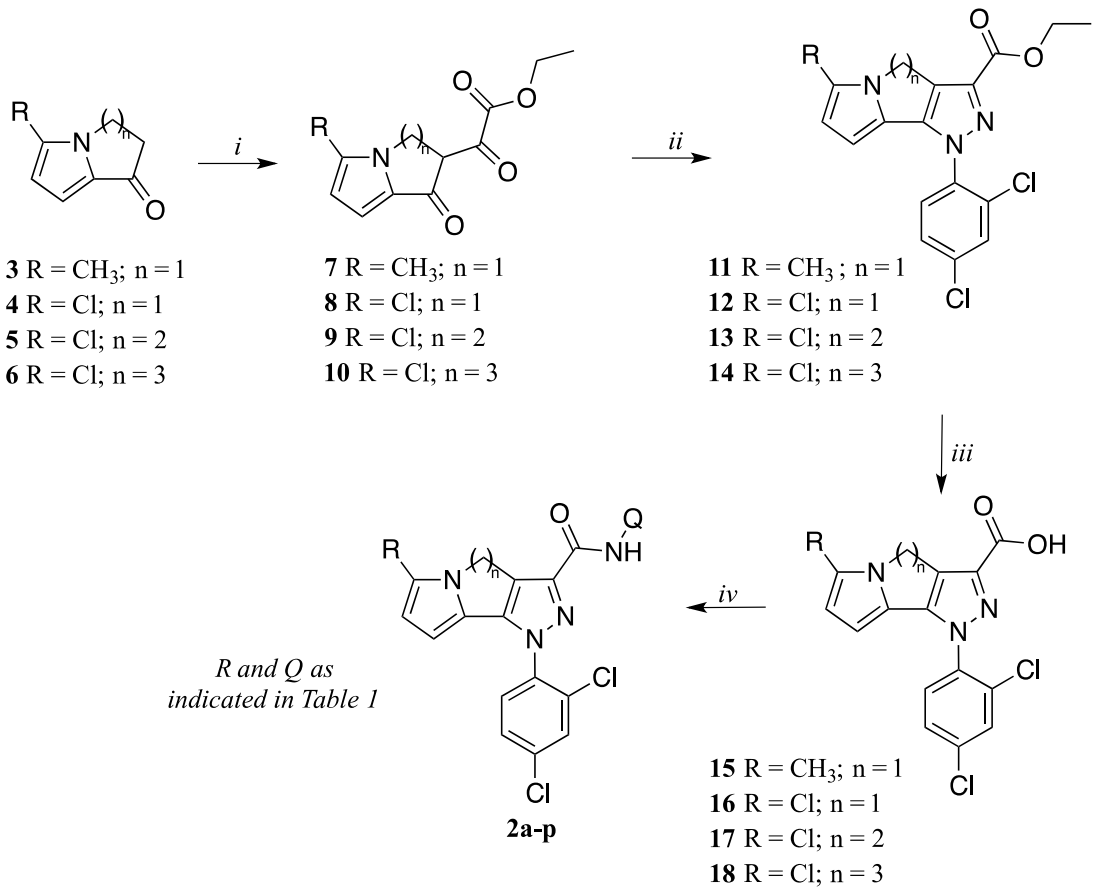

3 R = CH_3; n = 1
4 R = Cl; n = 1
5 R = Cl; n = 2
6 R = Cl; n = 3

7 R = CH_3; n = 1
8 R = Cl; n = 1
9 R = Cl; n = 2
10 R = Cl; n = 3

11 R = CH_3 ; n = 1
12 R = Cl; n = 1
13 R = Cl; n = 2
14 R = Cl; n = 3

15 R = CH_3; n = 1
16 R = Cl; n = 1
17 R = Cl; n = 2
18 R = Cl; n = 3

2a-p

Scheme 1. Reagents and conditions: *(i)* Na, EtOH, $(COOEt)_2$, r.t., 1 h; (*ii)* 2,4-$Cl_2C_6H_3NHNH_2$•HCl, EtOH, 80 °C, 8 h; (*iii)* THF, LiOH 0.8M, 60 °C, 3 h; (*iv)* EDC, HOBt, CH_2Cl_2, rt, 1 h, then NH_2-Q, overnight.

Table 1. Structures and binding data for compounds **2a-p**.

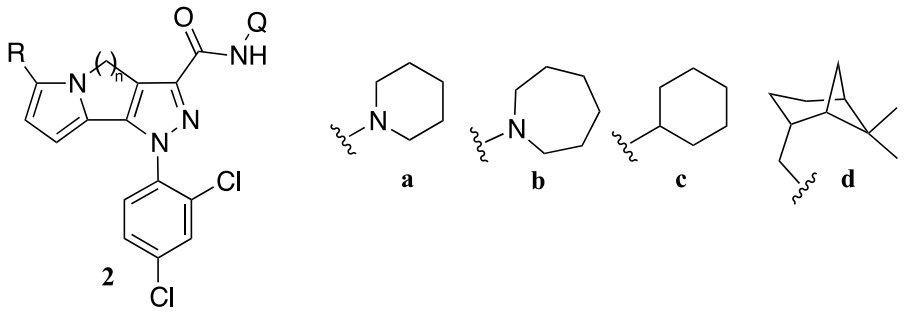

Compd.	R	n	Q	Receptor affinity		CB_1 selectivity
				$K_i CB_1$ (nM)[a]	$K_i CB_2$ (nM)[b]	$K_i CB_2/K_i CB_1$
2a	Cl	1	**a**	902	>1μM	>1.10
2b	Cl	1	**b**	230	615	2.67
2c	Cl	1	**c**	715	750	1.05
2d	Cl	1	**d**	355	314	0.88
2e	CH_3	1	**a**	>1μM	>1μM	–
2f	CH_3	1	**b**	895	>1μM	>1.11
2g	CH_3	1	**c**	>1μM	>1μM	
2h	CH_3	1	**d**	142	731	5.15
2i	Cl	2	**a**	209	>1μM	>4.78
2j	Cl	2	**b**	81	>1μM	>12.35
2k	Cl	2	**c**	154	>1μM	>6.49
2l	Cl	2	**d**	>1μM	>1μM	–
2m	Cl	3	**a**	190	>1μM	>5.26
2n	Cl	3	**b**	244	>1μM	>4.10
2o	Cl	3	**c**	544	958	1.76
2p	Cl	3	**d**	257	>1μM	>3.89

[a] Affinity of compounds for the CB_1 receptor was evaluated using mouse whole brain membranes and [^{3}H]CP 55,940. K_i values were obtained from five independent experiments carried out in triplicate.
[b] Affinity of compounds for the CB_2 receptor was evaluated using CHO cell membranes transfected with hCB_2 receptors and [^{3}H]CP 55,940. K_i values were obtained from five independent experiments carried out in triplicate.

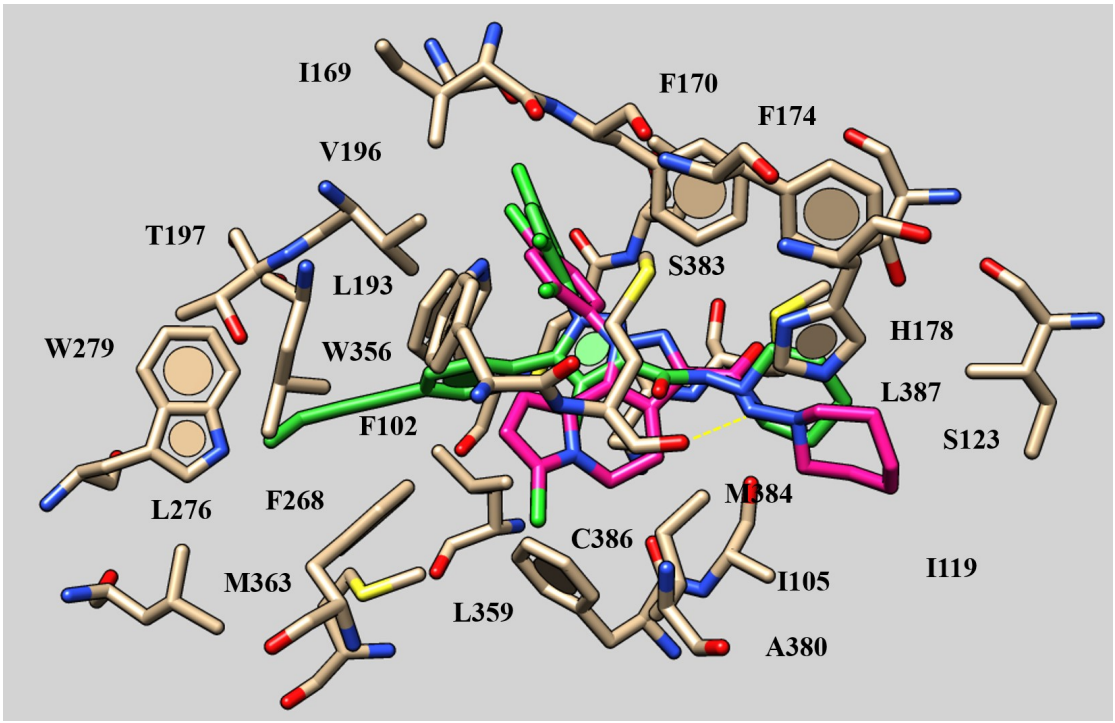

Figure 3. Docking mode of **2j** (C atom; magenta) within the X-Ray crystallographic coordinates of hCB_1 receptor in complex with AM6538 (C atom; green). The most important residues are labelled. H-bonds detected by the dihydropyrazolo[4,3-*g*]indolizine compound are shown by dot lines (in yellow).

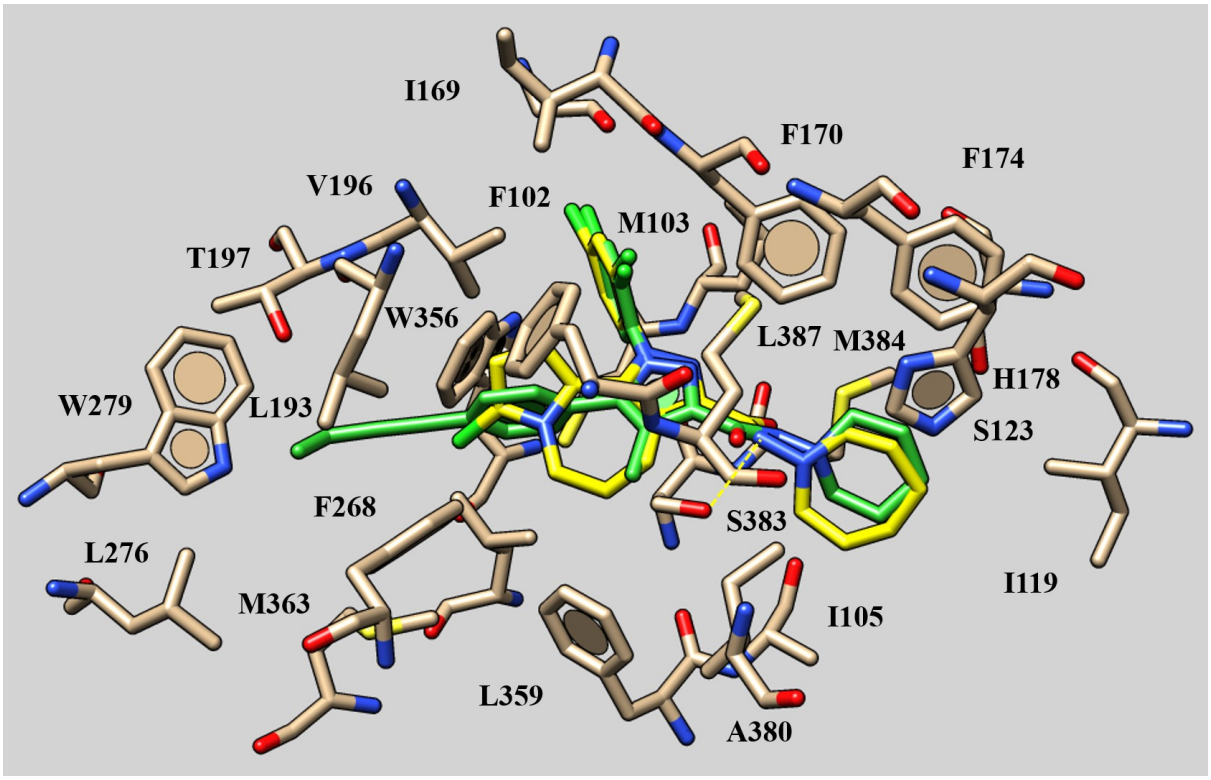

Figure 4. Docking mode of **2n** (C atom; yellow) within the X-Ray crystallographic coordinates of hCB_1 receptor in complex with AM6538 (C atom; green). The most important residues are labelled. H-bonds detected by the tetrahydropyrazolo[3,4-*c*]pyrrolo[1,2-*a*]azepine compound are shown by dot lines (in yellow).

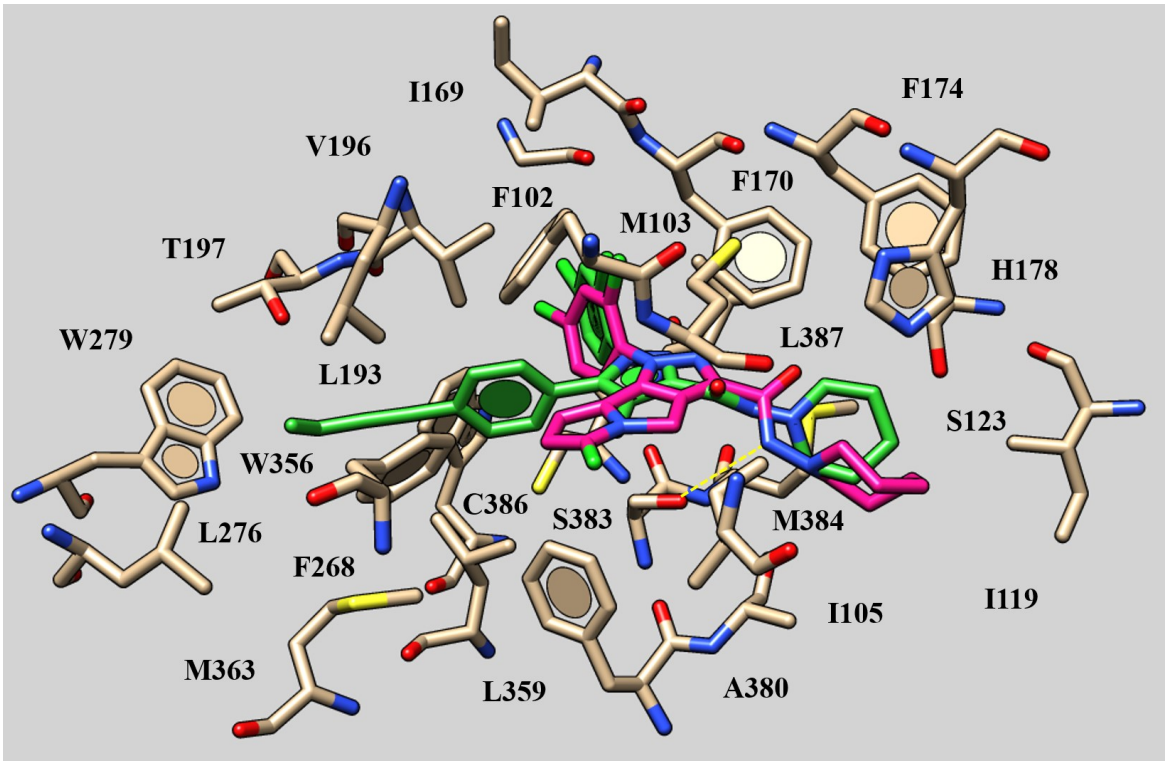

Figure 5. Docking mode of **2b** (C atom; magenta) within the X-Ray crystallographic coordinates of hCB_1 receptor in complex with AM6538 (C atom; green). The most important residues are labelled. H-bonds detected by the dihydropyrazolo[4,3-*g*]indolizine compound are shown by dot lines (in yellow).